Formation of Plasmoid Chains in Magnetic Reconnection

R. Samtaney,[1] N. F. Loureiro,[2] D. A. Uzdensky,[3] A. A. Schekochihin,[4] and S. C. Cowley[2, 5]

[1]*Princeton Plasma Physics Laboratory, Princeton University, Princeton, New Jersey 08543*
[2]*EURATOM/UKAEA Fusion Association, Culham Science Centre, Abingdon, OX14 3DB, UK*
[3]*Department of Astrophysical Sciences/CMSO, Princeton University, Princeton, New Jersey 08544*
[4]*Rudolf Peierls Centre for Theoretical Physics, University of Oxford, Oxford OX1 3NP, UK*
[5]*Plasma Physics, Blackett Laboratory, Imperial College, London SW7 2AZ, UK*
(Dated: March 3, 2009)

A detailed numerical study of magnetic reconnection in resistive MHD for very large, previously inaccessible, Lundquist numbers ($10^4 \leq S \leq 10^8$) is reported. Large-aspect-ratio Sweet-Parker current sheets are shown to be unstable to super-Alfvénically fast formation of plasmoid (magnetic-island) chains. The plasmoid number scales as $S^{3/8}$ and the instability growth rate in the linear stage as $S^{1/4}$, in agreement with the theory by Loureiro et al. [Phys. Plasmas **14**, 100703 (2007)]. In the nonlinear regime, plasmoids continue to grow faster than they are ejected and completely disrupt the reconnection layer. These results suggest that high-Lundquist-number reconnection is inherently time-dependent and hence call for a substantial revision of the standard Sweet-Parker quasi-stationary picture for $S > 10^4$.

PACS numbers: 52.35.Vd, 94.30.Cp, 96.60.Iv, 52.35.Py, 52.65.Kj

Introduction. Magnetic reconnection is a fundamental plasma process of rapid rearrangement of magnetic field topology, accompanied by a violent release of magnetically-stored energy and its conversion into heat and into non-thermal particle energy. It is of crucial importance for numerous physical phenomena such as solar flares and coronal mass ejections [1, 2], magnetic storms in the Earth's magnetosphere [3, 4, 5], and sawtooth crashes in tokamaks [6, 7]. Reconnection times in these environments are observed to be very short, usually only 10 to 100 times longer that the global Alfvén transit time, $\tau_A = L/v_A$, where L is the characteristic system size and v_A is the Alfvén speed. This is in direct contradiction with the classical Sweet-Parker (SP) [8, 9] reconnection model, which employs the simplest possible non-ideal description of plasma — two-dimensional (2D) resistive magnetohydrodynamics (MHD) — and predicts a very long reconnection time scale $\tau_{\rm rec} \sim \tau_A S^{1/2}$, where $S = Lv_A/\eta \gg 1$ is the Lundquist number, and η is the resistivity (or magnetic diffusivity) of the plasma. Both numerical simulations [10, 11] and laboratory experiments [12] have confirmed the SP theory for collisional plasmas where resistive MHD with smoothly varying (e.g., Spitzer) resistivity must apply. Because of this discrepancy between the MHD picture and observations, efforts to understand magnetic reconnection have moved beyond simple resistive MHD to increasingly sophisticated and realistic plasma-physics frameworks incorporating collisionless processes such as anomalous resistivity or two-fluid effects, where, indeed, fast reconnection rates have been found [13, 14]. For these reasons, simple resistive-MHD reconnection has come to be viewed as well understood, uninteresting, and mostly irrelevant.

However, most previous numerical studies of resistive MHD reconnection have been limited by resolution constraints to relatively modest Lundquist numbers ($S \sim 10^4$). The same is true for dedicated reconnection experiments. On the other hand, in most real applications of reconnection, the Lundquist numbers are much larger (e.g., $S \sim 10^{12}$ in the solar corona, $S \sim 10^8$ in large tokamaks). Thus, there is a large gap between the extreme parameter regime that we would like to understand and that accessible to the numerical and experimental studies performed so far. Asymptotically high values of S have never been probed by numerical simulations and, therefore, one cannot really claim a complete understanding of magnetic reconnection even in the simplest framework of 2D MHD with a (quasi-)uniform resistivity.

Of particular interest is the possibility that current sheets with large aspect ratios $L/\delta_{\rm SP} \sim S^{1/2}$, where $\delta_{\rm SP}$ is the width of the SP current layer, should be unstable and break up into chains of secondary magnetic islands, or plasmoids — a phenomenon absent from the SP theory. A tearing instability of large-aspect-ratio current sheets was anticipated by Bulanov et al. [15] and Biskamp [10]. Current sheets were, indeed, found to be unstable in those numerical experiments where $S \sim 10^4$ was reached (e.g. [10, 16, 17, 18, 19, 20]). Current-sheet instability and plasmoid formation have also been observed in numerical reconnection studies using other physical descriptions, e.g., fully kinetic simulations [21, 22, 23], and there is tentative observational evidence [24, 25] that they might play a key role in the dynamics of magnetic reconnection in the Earth magnetosphere and in solar flares. In fusion devices, plasmoid formation is less well diagnosed but recent results from the TEXTOR tokamak [26] suggest that they might also be present. Theoretically, plasmoid formation has been proposed as a mechanism of fast reconnection [19, 27] and non-thermal particle acceleration in reconnection events [23]. Thus, plasmoids

seem to be as ubiquitous as magnetic reconnection itself. However, even though their appearance has been reported by many authors, neither the plasmoid formation in the limit of asymptotically large S nor its effect on the reconnection process have been systematically investigated on any quantitative level and remains poorly understood.

As the first step towards this goal, Loureiro et al. [28] developed a linear theory of the instability of large-aspect-ratio current sheets that, unlike in the calculation of Ref. [15], emerges from a controlled asymptotic expansion in large S. Mathematically, the instability resembles a tearing instability with large Δ', leading to the formation of an inner layer with the width $\delta_{\rm inner} \sim S^{-1/8}\delta_{\rm SP}$. The instability is super-Alfvénically fast, with the maximum growth rate scaling as $\gamma\tau_A \sim S^{1/4}$; the fastest-growing mode occurs on a scale that is small compared to the length of the current sheet, viz., the number of plasmoids formed along the sheet scales as $S^{3/8}$.

In this Letter, we report the next logical step towards the detailed assessment of the role of plasmoids in magnetic reconnection: the first numerical evidence that not only do current sheets go unstable but that they do so in the extremely fast way predicted by Ref. [28] and the instability quantitatively obeys the scalings derived there. To this end, we perform a set of 2D MHD simulations of an SP reconnection layer with uniform resistivity and asymptotically large Lundquist numbers $10^4 \leq S \leq 10^8$.

Numerical Set Up. Probing such previously unattainable values of the Lundquist number is made possible by a special numerical set up that effectively zooms in on the SP current sheet by choosing a simulations box whose size in the direction across the reconnection layer (x) is just somewhat larger than, but generally tied to, the SP thickness, $L_x \gtrsim \delta_{\rm SP}$, while in the direction along the layer (y), the box covers a finite fraction of the global length L of the current sheet. The boundary conditions are used to mimic the asymptotic matching between the global and local solutions (in the spirit of [11]). Let us explain how this is done.

We solve the standard set of compressible resistive MHD equations (the adiabatic index is 5/3; viscosity and thermal conductivity are ignored) in an elongated 2D box, $[-L_x, L_x] \times [-L_y, L_y]$. At the upstream boundaries ($x = \pm L_x$), we prescribe the reconnecting component of the magnetic field, $B_y(x = \pm L_x, y) = \pm B_{\rm in}$ and the incoming velocity, $v_x(x = \pm L_x, y) = \mp v_{\rm in}$. As the box is understood to model an SP current sheet, we set $L_x = \delta_{\rm SP} = LS^{-1/2} = (L\eta/v_A)^{1/2}$, where v_A is the Alfvén speed corresponding to $B_{\rm in}$ and L is the (half-)length of the current sheet. We should then have $v_{\rm in} = v_A S^{-1/2} = (v_A\eta/L)^{1/2}$. We choose our code units so that $v_A = 1$ and $L = 1$. Then setting $L_x = \eta^{1/2}$ and $v_{\rm in} = \eta^{1/2}$ enforces a fixed SP reconnection rate based on $v_A = 1$ and $L = 1$. Choosing $L_y = 1$ would correspond to simulating the entire length of the current sheet, but

it is clear that in this local set up only an inner fraction of the sheet can be computed accurately, so we choose $L_y = 0.24$. At the downstream boundaries $y = \pm L_y$, free outflow boundary conditions are imposed. The method of characteristics is used to determine the remaining boundary conditions. Compressibility effects are minimized by ensuring that the Mach number $M = v_A/c_s$, where c_s is the sound speed, is small (in our simulations, it never exceeds 0.1). The initial conditions are chosen so as to represent qualitatively an SP-like current layer (using the Harris sheet profiles). We do not choose an initial perturbation with a particular wave number; instead the system itself is allowed to pick the most unstable wave number.

Time Evolution of the Instability. For $S < 10^4$, the current density at $x = 0$ settles down to a quasi-steady state, and no plasmoids are observed, consistent with SP theory. As the Lundquist number is increased, this picture changes dramatically. The system does not settle into a steady state — instead, as predicted by the linear theory [28], the layer becomes unstable and secondary islands (plasmoids) form, with reconnection occurring at multiple X-points. This is illustrated in Fig. 1, where the time evolution of the current density for $S = 10^7$ is shown. We see that a plasmoid chain develops along the sheet and also that the plasmoids closer to the center of the sheet grow faster than those farther away from it. In Fig. 3, we show the time evolution of the width of the plasmoid closest to the center of the sheet. At early times, it grows exponentially. The growth rates for different values of S are plotted in Fig. 4. The scaling $\gamma\tau_A \sim S^{1/4}$ predicted by the linear theory [28] is obeyed extremely well. The fact that the growth rate for the off-center plasmoids is a decreasing function of the distance along the sheet was not captured in the simple equilibrium model used in Ref. [28] but it does emerge in the calculation for a general SP equilibrium [29].

The linear stage ends when the plasmoid width exceeds the width of the inner layer, $\delta_{\rm inner} \sim S^{-1/8}\delta_{\rm SP}$ (see Fig. 3). The subsequent nonlinear growth is slower, but still sufficiently rapid to permit the plasmoids to reach the width of the current sheet before being advected out by the mean outflow along the SP sheet, $v_y \sim (y/L)v_A$. That this outflow causes the plasmoids to drift outwards is illustrated by Fig. 5, where we plot the time traces of the plasmoid O points along the sheet. The plasmoids that are further away from the center of the sheet move faster due to faster outflow. Note that new O-point traces appear in between already existing ones — we interpret this as evidence of secondary-plasmoid generation, arising from the collapse of the X points between the primary plasmoids into secondary current sheets, which then go unstable (cf. [18]). The breaking of the secondary sheets is also visible in the last two frames of Fig. 1. In some cases, we have also observed coalescence of nearby plasmoids (not shown).

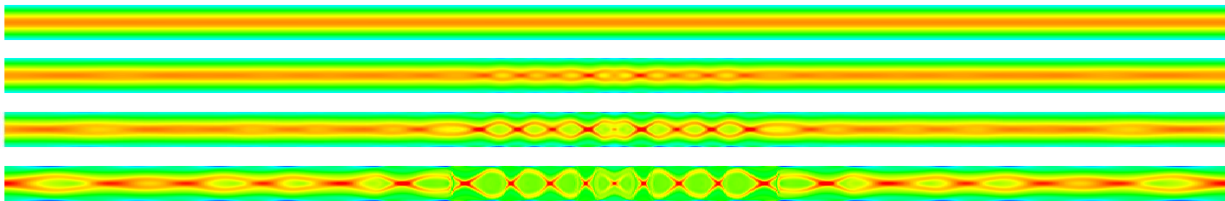Once the plasmoids grow enough to touch the wall,

FIG. 1: Contour plots of the current density showing the time evolution of an SP current sheet for $S = 10^7$. The times shown are, from top to bottom, $t = 0.63\tau_A$, $t = 0.96\tau_A$, $t = 1.09\tau_A$ and $t = 1.27\tau_A$. The domain shown is $-\delta_{\rm SP} \leq x \leq \delta_{\rm SP}$ (inflow direction, vertical), and $-0.12L \leq y \leq 0.12L$ (outflow direction, horizontal), where $\delta_{\rm SP} \simeq 3 \times 10^4$ is the SP layer width and $L = 1$ is the (half-)length of the current sheet (see text; only the central half of the simulation box is shown).
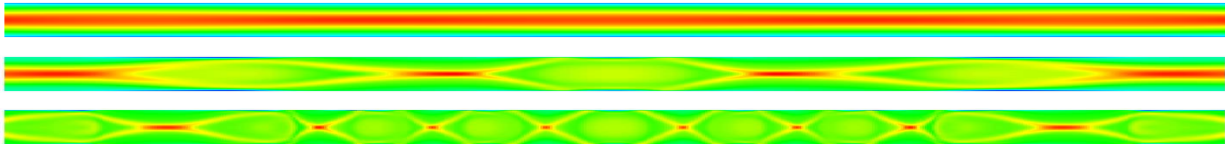
FIG. 2: Contour plots of the current density for (from top to bottom) $S = 10^4$ ($t = 4.5\tau_A$), $S = 10^5$ ($t = 2.9\tau_A$) and $S = 10^6$ ($t = 2.6\tau_A$); the case $S = 10^7$ is shown in Fig. 1.

the simulation becomes invalid and is stopped. The fact that they do touch the wall means that in a more general global set up, they would grow to exceed the SP width $\delta_{\rm SP}$, so the current sheet is broken up.

Spatial Structure of the Plasmoid Chain. The development of multiple magnetic islands for different values of S is illustrated in Fig. 2: an increasing number of plasmoids is observed as the Lundquist number increases. Fig. 6 shows the number of plasmoids vs. S. Again, there is excellent agreement with the scaling $\sim S^{3/8}$ of the most unstable wave number predicted by the linear theory [28]. Note that to avoid possible boundary-condition effects, we only count the number of plasmoids present in the central half of the simulation domain, $-0.12L < y < 0.12L$.

Note that the decrease in the linear growth rate with

y means that in practice the simulation must be run into a nonlinear state to observe the formation of the entire plasmoid chain. However, by the time the outer plasmoids become detectable (but still linear), the more central plasmoids can already be well into their nonlinear evolution, so some secondary plasmoid generation (and, in some cases, coalescence) might have already taken place. This means that there is a degree of imprecision in measuring the number of the primary plasmoids resulting from the linear instability of the entire current sheet (the diagnostic in Fig. 6 counts the maximum number of plasmoids during the run), especially at the largest values of S. However, the errors this introduces in Fig. 6 are not large and do not affect the validity of our claim that the theoretical scaling $S^{3/8}$ is obeyed. At even larger
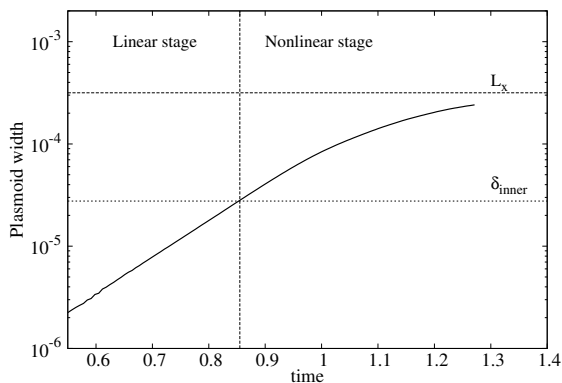

FIG. 3: Time evolution of the half-width of the plasmoid closest to the center of the sheet for $S = 10^7$. Half-widths of the inner layer, $\delta_{\rm inner}$ [28], and of the SP sheet, $\delta_{\rm SP} = L_x$, are shown for reference.
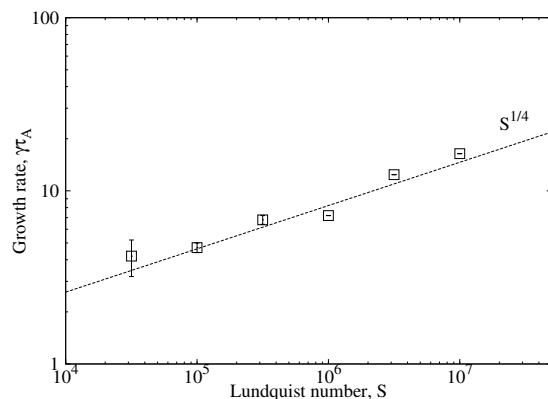

FIG. 4: The growth rate of the plasmoid closest to the center of the sheet vs. S. The theoretical slope $S^{1/4}$ [28] is shown for reference. For $S > 10^7$, we could not calculate the growth rates accurately because the linear regime was too short lived.
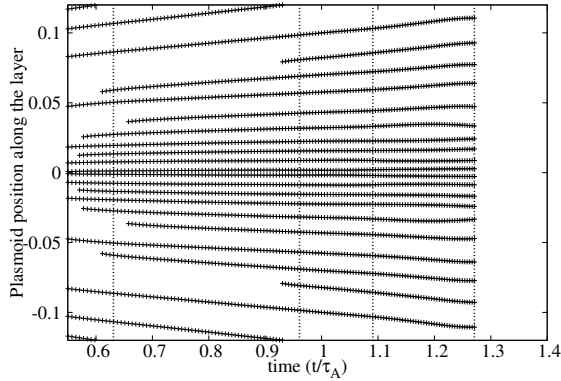
FIG. 5: Plot of the position of the O points vs. time for $S = 10^7$. Dotted lines mark the times at which the current sheet is shown in Fig. 1.

Lundquist numbers $S > 10^8$, the dynamics along the sheet is likely to be even messier, so a statistical description of plasmoid chains may be required (cf. [19, 27]).

Discussion. The key questions that remain to be answered are how large the plasmoids grow after they exceed the width of the SP layer, and what is their impact on the overall reconnection rate. Addressing these questions requires global (or, at least, intermediate-scale) simulations capturing regions both interior and exterior to the current sheet. We could not computationally afford such simulations and simultaneously resolve the very large values of S required to diagnose the current-sheet instability in its asymptotic form. In our view, it was important, before undertaking a global reconnection study, to understand the nature of the instability. The conclusion of this Letter is that the instability exists, is super-Alfvénically fast (cf. [20, 22]) and, in the limit of large S, quantitatively follows the linear theory of Ref. [28, 29]. We stress that this is the first numerical study that has been able to make this statement and thus, in a sense, demystify the phenomenon of multiple-plasmoid genera-
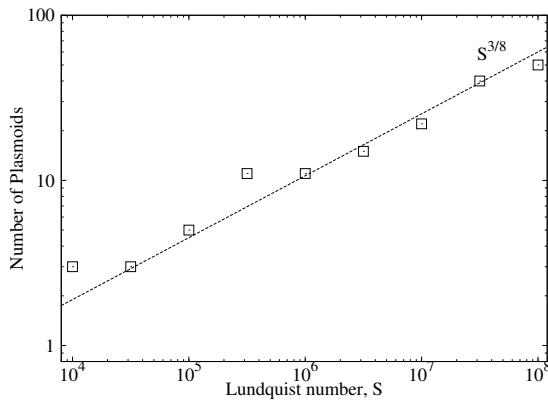
tion. This conclusion puts further investigations of the plasmoid effect on magnetic reconnection on a firm theoretical footing.

The body of numerical evidence for plasmoids is now so overwhelming that there should remain little doubt of their importance in reconnection processes. It is clear that for sufficiently large systems, plasmoid-dominated reconnection layers are inevitable. Plasmoid formation and magnetic reconnection are thus inextricably linked and further progress in understanding reconnection in realistic systems necessarily requires a theory that takes the plasmoid dynamics into account. It also requires experimental evidence — however, present-day magnetic reconnection experiments have not yet been able to observe plasmoid formation, most likely because of the moderate current sheet aspect ratios. The effect of plasmoids on reconnection is, in our view, one of the natural objects of emphasis for the next generation of dedicated magnetic reconnection experiments.

FIG. 6: The maximum number of plasmoids in the central part of the sheet, $-0.12L \leq y \leq 0.12L$, vs. S. The theoretical slope from linear theory, $S^{3/8}$ [28], is shown for reference.

[1] P. A. Sweet, Annu. Rev. Astron. Astrophys. **7**, 149 (1969).
[2] T. Yokoyama et al., Astrophys. J. **546**, L69 (2001).
[3] J. Dungey, Phys. Rev. Lett. **6**, 47 (1961).
[4] A. Bhattacharjee, Annu. Rev. Astron. Astrophys. **42**, 365 (2004).
[5] C. J. Xiao et al., Nature Phys. **2**, 478 (2006).
[6] M. Yamada et al., Phys. Plasmas **1**, 3269 (1994).
[7] R. J. Hastie, Astrophys. Space Sci. **256**, 177 (1997).
[8] P. A. Sweet, in *Electromagnetic Phenomena in Cosmical Physics*, edited by B. Lehnert (Cambridge University Press, Cambridge, 1958), p. 123.
[9] E. N. Parker, J. Geophys. Res. **62**, 509 (1957).
[10] D. Biskamp, Phys. Fluids **29**, 1520 (1986).
[11] D. A. Uzdensky and R. M. Kulsrud, Phys. Plasmas **7**, 4018 (2000).
[12] H. Ji et al., Phys. Plasmas **6**, 1743 (1999).
[13] M. Ugai and T. Tsuda, J. Plasma Phys. **17**, 337 (1977).
[14] J. Birn et al., J. Geophys. Res. **106**, 3715 (2001).
[15] S. Bulanov, J. Sakai, and S. Syrovatskii, Sov. J. Plasma Phys. **5**, 157 (1979).
[16] L. C. Lee and Z. F. Fu, J. Geophys. Res. **91**, 6807 (1986).
[17] S.-P. Jin and W.-H. Ip, Phys. Fluids B **3**, 1927 (1991).
[18] N. F. Loureiro et al., Phys. Rev. Lett. **23**, 235003 (2005).
[19] G. Lapenta, Phys. Rev. Lett. **100**, 235001 (2008).

[20] L. Ni, A. Bhattacharjee, and H. Yang, in preparation (2009).

[21] W. Daughton, J. Scudder, and H. Karimabadi, Phys. Plasmas **13**, 07201 (2006).

[22] W. Daughton et al., submitted to Phys. Rev. Lett. (2009).

[23] J. F. Drake et al., Geophys. Res. Lett. **33**, L13105 (2006).

[24] J. Lin, S. R. Cranmer, and C. J. Farrugia, J. Geophys. Res. **91**, 6807 (2008).

[25] A. Bemporad, Astrophys. J. **584**, 689 (2008).

[26] Y. Liang et al., Nucl. Fusion **47**, L21 (2007).

[27] K. Shibata and S. Tanuma, Earth Planets Space **53**, 473 (2001).

[28] N. F. Loureiro, A. A. Schekochihin, and S. C. Cowley, Phys. Plasmas **14**, 100703 (2007).

[29] N. F. Loureiro et al., submitted to Phys. Plasmas (2009).